Report 1

Reply to Anonymous Referee #3

The manuscript addresses an important topic in multi-angle polarimetric aerosol retrieval and makes use of valuable DPC observations. However, in its current form, the study exhibits substantial shortcomings in the justification of novelty, the description and reproducibility of the retrieval methodology, and the physical interpretation of several key results. In particular, the uncertainty characterization and its consistency with the assumed measurement accuracy are insufficiently addressed, and some systematic features in the retrieval products remain unexplained. These issues are considered fundamental and would require major methodological restructuring rather than incremental revision. I therefore recommend rejection of the manuscript in its present form. Specific comments are provided below to clarify the main concerns and to explain in more detail the basis for this recommendation.

The authors thank the reviewer for the detailed comments and thoughtful suggestions, which are very helpful in improving the manuscript. We have carefully considered all the comments and revised the manuscript accordingly. A detailed point-by-point response to these comments is presented below.

1. L47: “However, existing aerosol retrievals based on DPC observations have primarily focused on AOD.” This statement is not valid. A large number of studies have already used DPC observations to retrieve aerosol optical properties beyond AOD.

We thank the reviewer for this correction. We agree that several studies have already retrieved aerosol optical properties beyond AOD from DPC observations using physical inversion methods and machine learning approaches. Our original statement was not sufficiently precise. Our intention was to emphasize that SSA retrievals specifically from DPC/GaoFen-5 observations, especially at global scales, remain relatively limited, and the

currently available studies still have constraints (e.g., regional scope, surface-type limitation, or limited SSA accuracy).

To make this clear, we revisited the relevant literature and revised the text accordingly. Specifically, (1) Dong et al. (2024) retrieved SSA using a machine-learning approach, but the retrieval is limited to land conditions; (2) Fang et al. (2022) reported regional SSA retrieval rather than global SSA; and (3) Jin et al. (2024), Ji et al. (2025), and Zhang et al. (2025) reported SSA retrievals based on DPC-2/GaoFen-5(02) observations. Because DPC-2/GaoFen-5(02) differs from DPC/GaoFen-5 in instrument design and in temporal coverage, these results are not directly comparable to SSA retrieval from DPC/GaoFen-5, and therefore do not resolve the limited evidence for global SSA retrieval based on DPC/GaoFen-5 observations.

Based on this survey, we have revised the expression in L47-58 to avoid suggesting that DPC-based retrievals focus only on AOD, while correctly stating that SSA retrievals from DPC/GaoFen-5 remain less reported at global scales:

> *Many aerosol retrieval studies based on DPC/GaoFen-5 observations have reported high-quality AOD retrievals (with correlation coefficients up to 0.9 against ground-based measurements). Several studies have also extended the retrieval to additional aerosol optical properties, including SSA…Nevertheless, compared with AOD, SSA retrievals based on DPC/GaoFen-5 observations have been less frequently reported at large spatial scales, and studies that provide global SSA retrieval remain relatively limited.*

2. L55: "while numerical methods have so far been limited to regional and oceanic applications." This statement is not correct. DPC observations have already been used to retrieve aerosol parameters over land and at the global scale. Please add recent references related to aerosol retrievals using DPC observations. In addition, "This highlights the need for further exploration of global SSA retrieval using DPC observations" is also not valid, as global SSA retrievals based on physical methods and DPC observations have already been reported.

We thank the reviewer for this correction. We agree that our original expression was not accurate. Physically based numerical inversion methods using DPC observations have been applied for global aerosol retrievals (especially for AOD). Our intention was to emphasize that, compared with AOD, global-scale SSA retrievals from DPC based on physical methods are still relatively limited, and existing studies often focus on specific regions or over ocean.

After re-checking the recent literature, we found that while global aerosol retrievals from DPC observations using physical methods have indeed been reported (primarily focusing on AOD and related parameters), we did not identify a clearly documented study that performs global SSA retrieval using a physically based inversion method specifically with DPC/GaoFen-5 observations. Some global SSA retrieval studies exist but are based on different sensors. For example, Zhang et al. (2025) implemented the RemoTAP method for global SSA retrieval over land, but it was conducted using DPC-2/GaoFen-5(02) data rather than DPC/GaoFen-5. Given differences in instrument design and temporal coverage, those results are not directly comparable to a global SSA retrieval based on DPC/GaoFen-5 observations.

Therefore, we revised the text in L57-59 to remove the misleading statement and to avoid implying that global SSA retrievals do not exist:

> *On the other hand, studies applying physically based inversion methods to DPC observations for global SSA retrieval are still relatively limited. Further efforts are therefore needed to extend such physically based approaches on the global scale.*

3. L63: "This study uses measurements from the first DPC sensor since data is not well calibrated for the following two sensors." This statement is unclear. Which sensor is referred to as the "first DPC sensor"?

We thank the reviewer for pointing it out. In this study, the "first DPC sensor" refers to the DPC instrument onboard the Gaofen-5 satellite launched in May 2018. We have revised the manuscript in L70 to clarify:

This study uses measurements from the DPC instrument onboard the Gaofen-5 satellite launched in May 2018, as the data from the subsequent DPC instruments onboard Gaofen-5(02) and Daqi-1 are not yet well calibrated.

4. L68: What do you mean by "instrumental drift" in this context?

Thank you for the comment. In this study, "instrumental drift" refers to a gradual change in the radiometric response of the DPC sensor after launch. This drift is mainly attributed to aging and degradation of the optical system in the space environment, rather than changes in the detectors. As a result, the measured TOA radiance for the same target can slowly shift over time, leading to increasing radiometric biases if no correction is applied. This drift is known to be dependent on both wavelength and field of view (FOV, or viewing geometry), with a stronger sensitivity decrease at shorter wavelengths and larger variations across the FOV, as reported by Zhu et al. (2022). We have revised the expression in the manuscript in L79-81 to clarify:

However, after launch, DPC exhibited a gradual change in radiometric sensitivity, primarily due to aging of the optical components. This drift is dependent on both wavelength and field of view and can introduce increasing systematic biases if not properly corrected.

5. L70: What does "Rayleigh scattering-based" refer to?

Thank you for this comment. The term "Rayleigh scattering-based" refers to a radiometric calibration method developed by Zhu et al. (2022) which is based on the atmospheric Rayleigh scattering over deep ocean regions. In these areas with very low aerosol loading and low surface reflectance, the TOA radiance observed by the satellite is dominated by Rayleigh scattering, which can be accurately simulated using a Radiative Transfer Model (RTM). Zhu et al. (2022) quantified differences of DPC observed and RTM simulated radiances over these deep ocean regions, and derived monthly VZA-dependent calibration coefficients. In this study, these coefficients are applied to correct DPC radiance observations in order to reduce radiometric biases before aerosol and surface property retrievals. We have revised the manuscript to better describe the calibration procedure in L82-89.

The radiometric response of DPC/GaoFen-5 is progressively drifting over time and is realted to VZA. Zhu et al. (2022) developed a method based on Rayleigh scattering over the ocean to correct this drift. In deep ocean regions with very low aerosol loading and low surface reflectance, the TOA radiance observed by satellite sensors is dominated by atmospheric Rayleigh scattering, which can be accurately simulated using radiative transfer models. By comparing simulated radiances with DPC observations over such regions, Zhu et al. (2022) provided monthly VZA-dependent calibration coefficients at 443, 490, 565, and 670 nm. The calibration uncertainties are about 1-7 % (depending on the wavelength and VZA). In this study, these Rayleigh scattering-based calibration coefficients are applied to correct DPC's scalar reflectance at 443, 490, 565, and 670 nm.

6. L76–77: "the screening of cloud/ice/snow pixels additionally employs the original measurements from the other bands." Why are uncalibrated measurements used for cloud/ice/snow screening? You mentioned that the uncertainty of DPC observations may exceed 20%. Please quantify the retrieval errors introduced by not using calibration coefficients. You did not specify which calibration coefficients were used for the polarization measurements. First, please clearly state whether calibration coefficients were applied and provide their values. Second, if no calibration coefficients were used, please quantitatively assess the retrieval errors caused by ignoring calibration.

Thank you for this comment. We clarify that radiometric calibration was applied only to the scalar reflectance of the four retrieval bands (443, 490, 565, and 670 nm), because existing calibration studies for DPC/ GaoFen-5 have so far provided coefficients only for these four bands. For the other scalar bands and for all polarization observations, calibration coefficients were not applied because reliable post-launch calibration information (including coefficients) is currently unavailable.

The cloud/ice/snow screening also relies on the 865 nm observations as well as polarimetric reflectance, and these inputs therefore come from the original (uncalibrated) measurements. We acknowledge that uncalibrated data may affect screening performance, leading to either over-screening or residual cloud contamination. To reduce the risk of retaining cloudy

pixels, we adopted more conservative thresholds. For example, given that the uncertainty at 865 nm can be as large as ~23%, we increased the screening threshold by 20%. Over land, the criterion (R_{865}/R_{443}) was adjusted from 1.2 to 1.44. This tightening is intended to maintain robust cloud removal even when the uncalibrated 865 nm reflectance is positively biased.

Finally, the impact of ignoring calibration is mainly indirect because the retrieval itself uses only the four calibrated scalar bands. The resulting error is introduced through screening, i.e., by changing the balance between residual cloud contamination and the loss of valid clear pixels.

7. L92: "The AOD measurements can be obtained at several wavelengths ranging from 340 nm to 1640 nm." AERONET does not appear to provide AOD measurements at 1640 nm.

Thank you for the comment. AERONET does provide AOD measurements at 1640 nm for sites equipped with Cimel sun photometers that include an InGaAs detector. As described by Giles et al. (2019), the nominal standard AERONET aerosol wavelengths include 340, 380, 440, 500, 675, 870, 1020, and 1640 nm. The availability of the 1640 nm channel depends on the instrument configuration at a given site, and therefore not all AERONET stations provide measurements at this wavelength.

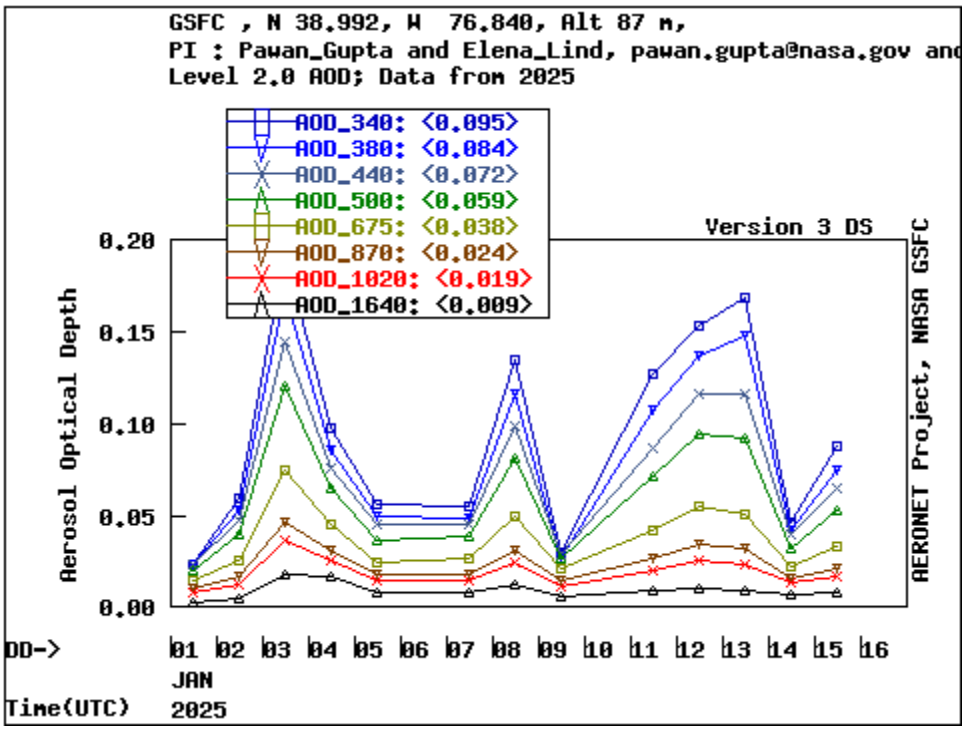

Fig. R1-1. AERONET Level 2.0 daily AOD observations at the GSFC site for January 2025. The figure is provided by NASA, downloaded from https://aeronet.gsfc.nasa.gov/ on 6 February 2026.

As an illustration, Fig. R1-1 shows Level 2.0 AOD data for January 2025 from the AERONET GSFC site (downloaded from the AERONET website), which include valid observations at 1640 nm. We agree that the original wording may imply that all AERONET sites provide AOD at 1640 nm, and we have revised the manuscript in L105 to clarify:

> *The AOD measurements are available at multiple wavelengths ranging from 340 to 1640 nm, depending on the site and instrument configuration, whereas the SSA products are provided at four wavelengths at 440, 675, 870 and 1020 nm.*

8. L96–97: "we utilize the all-point Version 3 Level 2.0 direct AOD measurements." This statement is unclear. Does "direct AOD" mean that the AOD is not quality-controlled? What does "all-point" refer to?

Thank you for the comment. The "direct AOD" refers to aerosol optical depth retrieved from direct-sun observations of the AERONET sun photometer, as opposed to AOD products derived from sky-radiance inversions. It does not indicate that the data are

unprocessed. The Version 3 Level 2.0 AERONET AOD data used here have undergone standard cloud screening and quality control.

The term "all-point" refers to the original temporal resolution of the AERONET observations, i.e., individual measurement points for each observation time. The "all-point" data is a product provided by AERONET, in contrast to those temporally aggregated products such as daily-mean or monthly-mean data.

We have revised the manuscript in L109-112 to clarify:

> *Considering the data quality and data availability, this study utilizes the Version 3 all-point (individual measurement) Level 2.0 AERONET AOD data derived from direct-sun observations, along with quality-controlled Level 1.5 almucantar SSA retrievals from sky radiance measurements.*

9. In Eq. (4), the cost function of the retrieval algorithm is given, but the state vector to be retrieved and the prior information are not specified.

Thank you for this comment. We agree that the state vector and the prior information should be specified. In the revised manuscript, we have clarified the composition of the state vector, a priori estimates, and the associated errors in Sect. 2.6.

Specifically, the state vector has been described as a combination of aerosol and surface parameters (L180-189):

> *The state vector, $\boldsymbol{x}$, is composed of aerosol and surface parameters. Particularly, for land surfaces, the state vector $\boldsymbol{x}$ consists of AOD ($\tau(\lambda)$), SSA ($\omega(\lambda)$), kernel intensity parameters of RTLS model ($K(\lambda)$, k_{vol}, and k_{geo} in Eq. 2), and the scale factor of BPDF-NDVI model (C in Eq. 8)…For water surfaces, only $\tau(\lambda)$ and $\omega(\lambda)$ are retrieved as components of the state vector $\boldsymbol{x}$, and the New Cox-Munk model is implemented to compute the surface reflectance (Spurr, 2006). The wavelength-dependent parameters, $\tau(\lambda)$, $\omega(\lambda)$, and $K(\lambda)$, are retrieved at 443, 490, 565, and 670 nm, corresponding to the wavelengths at which DPC observations are used to construct the measurement vector.*

The description of a priori values and the corresponding uncertainties has also been clarified in L189-192:

> *For AOD and SSA, the a priori state vector and its associated error covariance matrix are prescribed as fixed values, derived from the mean and variance of AERONET measurements. The a priori estimates of surface properties are also fixed, with their errors defined by the corresponding ranges of variability.*

We have also added a table (Table 3) summarizing the state vector and the associated prior information.

10. Section 3.1: What SSA value is used in the simulations? Under different SSA conditions, a ±0.03 perturbation may lead to completely different conclusions. Moreover, the apparent reflectance change induced by SSA perturbations does not seem equivalent to the accuracy required for satellite aerosol retrievals.

Thank you for this comment. In the original manuscript, the SSA used in Sect. 3.1 was computed using a Mie code (Mishchenko et al., 1999), based on the refractive index and particle size distribution of the moderately absorbing aerosol type (Levy et al., 2007). Specifically, the baseline SSA decreases slightly with wavelength, from 0.94 at 443 nm to 0.92 at 865 nm, and the sensitivity tests in Sect. 3.1 were conducted by perturbing SSA around this spectral baseline.

In the revised manuscript, we expanded the SSA range to 0.8-1.0. We also examined whether the same SSA perturbation produces comparable changes in I and DOLP at different SSA levels (Fig. R1-2). The results show that changing SSA from 0.8 to 0.84 (Fig. R1-2a,b) and from 0.96 to 1.0 (Fig. R1-2c,d) leads to broadly similar variations in I and DOLP. Therefore, under different SSA conditions, the impacts of the same perturbation are likely to be similar.

We also agree that the current observation accuracy is not sufficient to resolve the small changes in I and DOLP induced by 0.03 SSA perturbations. As a result, SSA retrievals based on DPC measurements can have large uncertainties, which is consistent with the relatively large errors reported in existing SSA products.

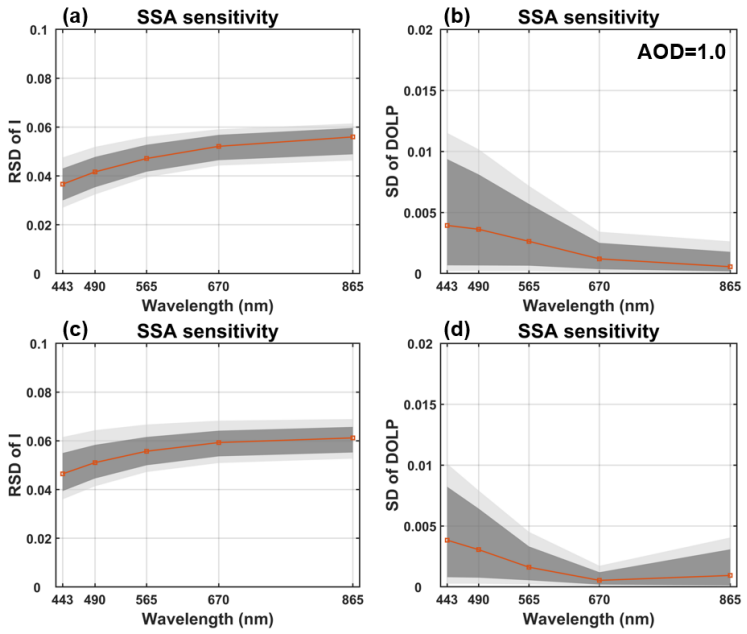

Fig. R1-2. Relative standard deviation (RSD) of I (a, c) and standard deviation (SD) of DOLP (b, d) induced by variations in SSA under different SSA levels. SSA varies from 0.80 to 0.84 in (a, b), and from 0.96 to 1.00 in (c, d).

11. In Fig. 5, please explain why AOD and DHR are simultaneously underestimated under high aerosol loading conditions. In addition, why do the numbers of retrieved AOD values differ among different wavelengths?

Thanks for this insightful comment. The underestimation observed under high aerosol loading conditions is not strictly simultaneous between AOD and DHR. By shading the AOD retrievals according to the DHR residual (Fig. R1-3(a)), we find that in part of the underestimated high-AOD cases, the retrieved DHR are overestimated, suggesting a compensation effect between surface reflectance and aerosol loading within the inversion framework. In addition, the AOD retrieval is also coupled with SSA. Under high aerosol conditions, underestimated AOD frequently corresponds to overestimated SSA (Fig. R1-3(b)), further reflecting parameter trade-offs in the retrieval process. Finally, the presence of residual errors in the retrieval is expected.

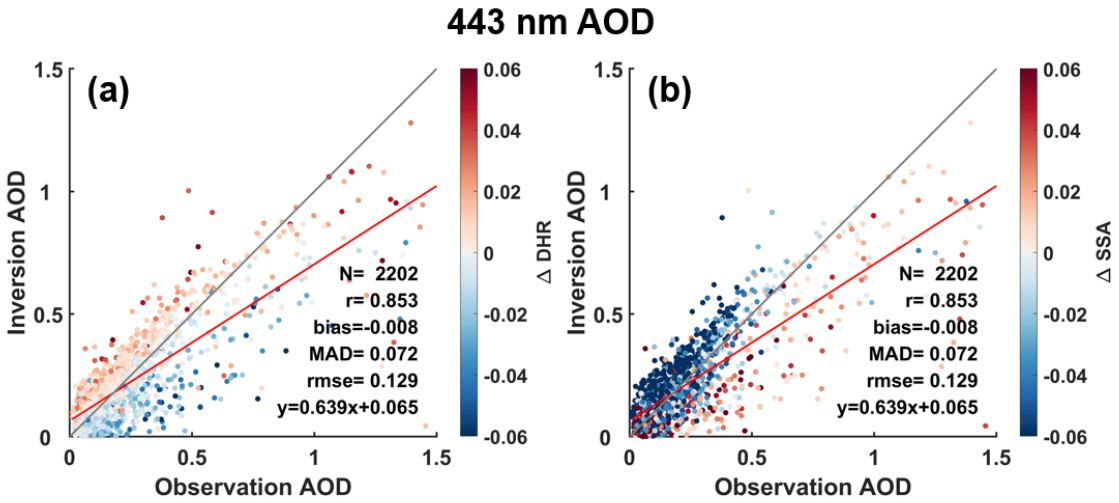

Fig. R1-3. Validation results of AOD at 443 nm. The points are shading to the (a) DHR residual (ΔDHR), and (b) SSA residual (ΔSSA).

As for the differing numbers of retrieved AOD values among wavelengths, this discrepancy originates from the previous quality control procedure based on single bands. In the original implementation, each wavelength was screened independently based on whether the retrieved parameters fell within the predefined ranges listed in Table 3. Retrievals located at the preset boundaries were regarded as less reliable and excluded, resulting in band-dependent sample sizes. In the revised manuscript, we have adopted a joint quality control strategy that evaluates all wavelengths involved in the inversion simultaneously, ensuring consistent sample selection across bands.

12. In Fig. 8, the map of AOD contains missing values, while SSA does not. Why?

We thank the reviewer for pointing this out. The missing values in the AOD map of Fig. 8 are mainly associated with cloud patches, which were correctly screened in the map of AOD. After careful examination, we found that during the spatial resampling step of the SSA image processing, these masked grids were not properly excluded due to a processing issue. This issue has been identified and fixed, and Fig. 8 has been updated accordingly in the revised manuscript.

13. Under biomass burning conditions, why do high SSA values overlap with possible aerosol plumes? Biomass burning is generally expected to emit strongly absorbing aerosols. Please explain.

We thank the reviewer for this important comment. Biomass burning aerosols are generally characterized by enhanced absorption and relatively low SSA. After carefully comparing the true-color image, AOD map, and SSA map, we note that the relatively high SSA values are mainly located at the edges of the smoke plumes, where AOD is comparatively low, rather than in the core areas of the plumes. On one hand, under low-AOD conditions, SSA retrieval becomes less constrained and exhibit higher uncertainty, and the solution is more sensitive to the assumed initial values. The SSA values in these regions (approximately 0.92–0.95) might be influenced by the selected initial settings. On the other hand, the SSA values in these regions are typically around 0.92–0.95, which does not indicate strongly scattering aerosols but rather moderate absorption. This is also consistent with possible mixing and aging effects near plume edges, which may increase SSA relative to the fresh plume core. This is in line with in situ observations reported by Kleinman et al. (2020), who found that near-fire aerosol had SSA of ~0.8-0.9, while after ~1-2 hours of aging SSA was typically ~0.9 or higher. We have clarified this point in the revised manuscript in L377:

> *The relatively higher SSA values are mainly located at the edges of the biomass-burning plumes, where AOD is relatively low and the SSA retrieval has larger uncertainty. In these regions, the retrieved SSA (typically around 0.92–0.95) is weakly constrained and therefore more sensitive to the assumed a priori values. Such SSA values suggest moderately absorbing aerosols and may reflect the influence of possible mixing and aging processes near the plume edges, consistent with Kleinman et al. (2020), who reported that near-fire smoke had SSA of ~0.8-0.9, while after ~1-2 h of aging SSA was typically ~0.9 or higher.*

To mitigate this issue, future improvements of the retrieval algorithm will consider incorporating spatiotemporal constraints to better stabilize SSA retrievals in such regions.

14. Fig. 9 shows similar issues to Fig. 8. The missing values of AOD and SSA do not overlap. In addition, irregular blank areas appear in coastal regions. Please explain the reasons.

We thank the reviewer for the comment. The missing values of AOD and SSA do not overlap because of the quality-control criteria applied to SSA. In particular, SSA retrievals are unreliable under low AOD conditions. Therefore, SSA values are screened when AOD falls below a predefined threshold (AOD<0.3), whereas the corresponding AOD values are retained. This explains the larger number of missing values in the SSA map, which are predominantly located in regions with low AOD.

The irregular blank areas in coastal regions have a different origin. In our retrieval, land and ocean pixels are treated using different surface parameterizations. However, coastal pixels cannot be clearly classified as either land or ocean under the current surface treatment. To avoid introducing large surface-related biases, these coastal pixels are excluded from the retrieval, resulting in irregular blank areas near coastlines.

We have also revised the manuscript in L387 to clarify:

Coastal pixels are excluded from the retrieval because they cannot be clearly classified as land or ocean, leading to missing values near coastlines. SSA values in low-AOD regions are also screened due to low reliability.

15. Please explain the anomalously high AOD values at high latitudes in Fig. 10(c) and over northwestern China in Fig. 10(d).

We thank the reviewer for this comment. By examining the retrieval results and true-color imagery for the corresponding periods, we found that these anomalously high AOD values are likely attributed to residual cloud contamination that was not completely removed by the cloud screening process. Particularly, in January 2020 (Fig. 10(d)), the affected regions show persistent, widespread thick cloud cover. In October 2019 (Fig. 10(c)), cloud cover is also frequently observed at high latitudes. This increases the likelihood of cloud contamination and can lead to artificially high AOD. In the revised manuscript, we have

applied a more rigorous cloud screening procedure to better suppress these cloud-related artifacts, and the corresponding figures have been updated accordingly.

16. Please explain the anomalously low SSA values over South America in Fig. 11(b) and over northern Asia in Fig. 11(c).

We thank the reviewer for this comment. The reason is the same as in the previous comment: the anomalously low SSA values are most likely related to residual cloud contamination. In the revised manuscript, we have applied a more rigorous cloud screening procedure, which reduces these low-SSA artifacts over South America (Fig. 11(b)) and northern Asia (Fig. 11(c)), and the figures have been updated accordingly.

17. Please add comparisons with other satellite aerosol products and provide global difference maps.

We thank the reviewer for this comment. In the revised manuscript, we have added regional MODIS AOD map during the pollution event in the manuscript. In addition, monthly global MODIS AOD maps and the corresponding global difference maps are provided in the Supplement. Related analysis and discussions have also been added into Sects. 3.4 and 3.5 to further evaluate our results.

18. Please explain the reason why AOD and DHR are simultaneously underestimated under high aerosol loading conditions.

Thank you for this comment. The underestimation under high aerosol loading is not strictly simultaneous between AOD and DHR. Analysis based on DHR differences indicates that, in part of the underestimated high-AOD cases, DHR is overestimated, suggesting a compensation effect between surface reflectance and aerosol loading within the inversion. Moreover, underestimated AOD under heavy aerosol conditions is often accompanied by overestimated SSA, further reflecting parameter trade-offs in the retrieval framework. A more detailed discussion is provided in our response to Comment #11.

19. Please correct the grammatical errors throughout the manuscript.

We thank the reviewer for this comment. We have carefully checked the manuscript and corrected the grammatical errors.

Reference

Dong, Y., Li, J., Zhang, Z., Zheng, Y., Zhang, C., & Li, Z. (2024). Machine learning-based retrieval of aerosol and surface properties over land from the gaofen-5 directional polarimetric camera measurements. *IEEE Transactions on Geoscience and Remote Sensing*, *62*, 1–15. https://doi.org/10.1109/tgrs.2024.3419169

Fang, L., Hasekamp, O., Fu, G., Gong, W., Wang, S., Wang, W., et al. (2022). Retrieval of aerosol optical properties over land using an optimized retrieval algorithm based on the directional polarimetric camera. *Remote Sensing*, *14*(18), 4571.

Giles, D. M., Sinyuk, A., Sorokin, M. G., Schafer, J. S., Smirnov, A., Slutsker, I., et al. (2019). Advancements in the aerosol robotic network (AERONET) version 3 database automated near-real-time quality control algorithm with improved cloud screening for sun photometer aerosol optical depth (AOD) measurements. *Atmospheric Measurement Techniques*, *12*(1), 169–209. https://doi.org/10.5194/amt-12-169-2019

Ji, Z., Li, Z., Zhang, Z., Fu, G., Hasekamp, O., Fan, C., et al. (2025). Retrieval of aerosol properties over the ocean using data from the second-generation directional polarization camera (DPC-2) onboard the GF-5(02) satellite. *Journal of Geophysical Research: Atmospheres*, *130*(17). https://doi.org/10.1029/2025jd043908

Jin, S., Ma, Y., Wang, Z., Hong, J., Chen, F., Ti, R., et al. (2024). Retrievals and performance assessment of global marine aerosol optical properties from DPC/GRASP. *Journal of Atmospheric and Environmental Optics*, *19*(6), 680–697.

Kleinman, L. I., Sedlacek III, A. J., Adachi, K., Buseck, P. R., Collier, S., Dubey, M. K., et al. (2020). Rapid evolution of aerosol particles and their optical properties downwind of wildfires in the western US. *Atmospheric Chemistry and Physics*, *20*(21), 13319–13341. https://doi.org/10.5194/acp-20-13319-2020

Levy, R. C., Remer, L. A., & Dubovik, O. (2007). Global aerosol optical properties and application to moderate resolution imaging spectroradiometer aerosol retrieval over land. *Journal of Geophysical Research: Atmospheres*, *112*(D13), D13210. https://doi.org/10.1029/2006jd007815

Mishchenko, M. I., Dlugach, J. M., Yanovitskij, E. G., & Zakharova, N. T. (1999). Bidirectional reflectance of flat, optically thick particulate layers: An efficient radiative transfer solution and applications to snow and soil surfaces. *Journal of Quantitative Spectroscopy and Radiative Transfer*, *63*(2-6), 409–432. https://doi.org/10.1016/s0022-4073(99)00028-x

Spurr, R. J. D. (2006). VLIDORT: A linearized pseudo-spherical vector discrete ordinate radiative transfer code for forward model and retrieval studies in multilayer multiple scattering media. *Journal of Quantitative Spectroscopy and Radiative Transfer*, *102*(2), 316–342. https://doi.org/10.1016/j.jqsrt.2006.05.005

Zhang, Z., Li, Z., Fu, G., Hasekamp, O., Fan, C., Qie, L., et al. (2025). Global aerosol retrieval over land using the chinese satellite polarimeter DPC-2/GF-5(02). *IEEE Transactions on Geoscience and Remote Sensing*, *63*, 1–14. https://doi.org/10.1109/tgrs.2025.3633391

Zhu, S., Li, Z., Qie, L., Xu, H., Ge, B., Xie, Y., et al. (2022). In-flight relative radiometric calibration of a wide field of view directional polarimetric camera based on the rayleigh scattering over ocean. *Remote Sensing*, *14*(5), 1211. https://doi.org/10.3390/rs14051211